Annals of Nuclear Medicine Vol. 14, No. 6, 467–476, 2000

Assessment of liver function in chronic liver diseases and regional function of irradiated liver by means of ^{99m}Tc-galactosyl-human serum albumin liver scintigraphy and quantitative spectral analysis

Akira FUKUI,* Kenya MURASE,** Takaharu TSUDA,*** Takashi FUJII*** and Junpei IKEZOE***

*Department of Radiology, Uwajima City Hospital
**Department of Medical Engineering, Division of Allied Health Science, Osaka University School of Medicine
***Department of Radiology, Ehime University School of Medicine

Scintigraphy with ^{99m}Tc-diethylenetriamine pentaacetic acid galactosyl human serum albumin (^{99m}Tc-GSA) was performed on 102 patients, then the hepatic extraction fraction (HEF), the rate constant for liver uptake of the tracer from the blood (K_1) and the hepatic blood flow index (HBFI) were determined by spectral analysis. The HEF, K_1 and HBFI values correlated moderately or closely with various indices of hepatic function, and the HEF and K_1 values decreased according to the stage of liver dysfunction. The HEF and K_1 values linearly and nonlinearly correlated with HH15 and LHL15, respectively. The HEF, K_1 and HBFI values for the irradiated portion of 20 patients before and after irradiation were compared. The HEF value in patients with a cirrhotic liver significantly ($p < 0.002$) decreased compared with that in patients with a normal liver at a dose of less than 40 Gy, whereas the HBFI value in patients with a normal liver significantly ($p < 0.05$) decreased compared with that in patients with a cirrhotic liver at a dose of 40 Gy or greater. This method appears to be a simple, non-invasive and useful tool with which to quantitatively evaluate liver function and it also helps clarify changes in regional function of the irradiated liver.

Key words: ^{99m}Tc-GSA, spectral analysis, liver function, regional function of irradiated liver

INTRODUCTION

THE ASIALOGLYCOPROTEIN (ASGP) receptor located exclusively on the surface of mammalian hepatocytes, is taken into these cells by binding to the ASGP receptor.[1–3] Technetium-99m-diethylenetriamine pentaacetic acid galactosyl human serum albumin (^{99m}Tc-GSA) is analogous to the ASGP receptor that is widely used to evaluate liver function, because the activity of the receptor decreases in various liver diseases.[4–6] Various methods have been devised with which to quantify liver function,[7–9] but they have not always been appropriate for routine clinical use because the procedures are complex. A simplified method with which to quantify liver function by means of ^{99m}Tc-GSA scintigraphy should be developed.

The spectral analysis introduced by Cunningham and Jones can be applied to dynamic positron emission tomography (PET) studies.[10] This technique is relatively simple, and various items of information, such as the spectrum of kinetic components representing the partitioning of tracer from the blood to the tissue and the unit impulse tissue response function, can be obtained with minimal modeling assumptions.[10] We developed a simplified method of quantitative ^{99m}Tc-GSA liver scintigraphy by means of spectral analysis.[11] Our method based on spectral analysis can provide the comprehensive and regional liver function by setting a ROI to a portion of the liver.

The effects of irradiation on the liver and changes in regional function at various doses of radiation have not been completely defined.[12,13] To apply safe radiation

Received August 3, 2000, revision accepted October 12, 2000.

For reprint contact: Akira Fukui, M.D., Department of Radiology, Uwajima City Hospital, 1–1 Gotenmachi, Uwajima, Ehime 798–8510, JAPAN.
E-mail: afukui@dr1.uwajima-mh.go.jp

Table 1 Correlations of the hepatic extraction fraction (HEF), the rate constant for the liver uptake of the tracer from the blood (K_1) and the hepatic blood flow index (HBFI) with liver functional tests

	n	HEF		K_1 (min^{-1})		HBFI (min^{-1})	
		r	p	r	p	r	p
KICG	94	0.737	< 0.0001	0.797	< 0.0001	0.647	< 0.0001
PT	84	0.484	< 0.0001	0.398	< 0.0002	0.268	0.0136
HPT	88	0.549	< 0.0001	0.543	< 0.0001	0.411	< 0.0001
T.B.	91	0.270	0.0096	0.365	0.0004	0.162	ns
T.P.	94	0.021	ns	0.109	ns	0.133	ns
Alb	92	0.452	< 0.0001	0.390	0.0001	0.280	< 0.0070
ChE	90	0.578	< 0.0001	0.580	< 0.0001	0.479	< 0.0001

HEF = hepatic extraction fraction; K_1 = rate constant for the liver uptake of the tracer from the blood; HBFI = hepatic blood flow index; KICG = plasma disappearance rate of indocyanine green; PT = prothrombin time; HPT = hepaplastin test; T.P. = total protein; Alb = albumin; ChE = cholinesterase; ns = not significant

therapy to the liver, liver damage due to irradiation should be determined. Our method should be able to separately evaluate hepatocyte function and hepatic blood flow in the irradiated liver.

The present study investigates the clinical applicability of our method based on spectral analysis to the assessment of liver function in patients with chronic liver diseases, and evaluates the effect of irradiation on the liver.

MATERIALS AND METHODS

Subjects

One hundred and two patients [58 males and 44 females; age, 65.5 ± 9.7 (mean ± SD) years] underwent ^{99m}Tc-GSA scintigraphy. Of these patients, sixty-two (32 males and 30 females; age, 63.3 ± 10.7 years) were divided into the following 4 groups, based on the clinical staging of hepatic functional capacity established by the Liver Cancer Study Group of Japan[14]: N (no history of liver disease, n = 13); I (mild dysfunction, n = 27); II (moderate dysfunction, n = 12) and III (severe dysfunction, n = 10) (Fig. 3).

Of the 102 patients, 20 (9 males and 11 females; age, 66.7 ± 10.4 years) were treated by radiation therapy for various malignant diseases, and their livers were partially included in the irradiation field. These patients were examined several times after irradiation with various doses of 4 Mv X-rays to the anterior/posterior or antero-posterior opposite portals. Their diseases were as follows: hepatoma, n = 6, cholangioma, n = 2, bone metastasis, n = 5, lymph node metastasis, n = 3, lung cancer, n = 1, esophageal cancer, n = 1, malignant lymphoma, n = 1, and leukemia, n = 1 (Table 2). Ten patients had undergone chemotherapy or chemoembolization therapy, and irradiation started after their biochemistry recovered. These 20 patients were divided into a normal liver group (no history of liver disease or good liver function, n = 13) and a liver cirrhosis group, n = 7 (Fig. 5). In a liver cirrhosis group of 7 patients, liver cirrhosis in 6 of the patients' was caused by the hepatitis C virus. The remaining case of cirrhosis was caused by the hepatitis B virus.

Informed consent was obtained from each patient after receiving an explanation of the purpose of this study and the scanning procedure.

Data acquisition

All patients received approximately 185 MBq of ^{99m}Tc-GSA (Nihon Medi-Physics, Nishinomiya, Japan) by means of a bolus injection into the peripheral vein, immediately followed by a saline flush. Before injection, the ^{99m}Tc-GSA was prepared by combining 1 molecule of human serum albumin with 30–44 molecules of galactose. Diethylenetriamine pentaacetic acid (DTPA) was used as a chelating agent for ^{99m}Tc labeling.

Sequential anterior images of the chest and upper abdomen were acquired in the supine position by means of a large-field-of-view gamma camera with a low energy, high resolution, parallel-hole collimator (GCA602A, Toshiba, Japan or Starcam4000, GE, United States) for 30 min at 1 min per frame in a 64 × 64 matrix.

Regions of interest (ROIs) were drawn over the whole liver and precordium. When analyzing the effect of irradiation to the liver, another ROI was drawn over the irradiated portion of the liver. Time-activity curves were then generated with these ROIs. The counts were normalized by scan length to obtain counts per $pixel^{-1}$ min^{-1} for a given ROI, and subsequently corrected for radioactive decay.

Spectral analysis

By means of spectral analysis,[10,11,15] we calculated the hepatic extraction fraction (HEF), the rate constant for liver uptake of the tracer from the blood (K_1, min^{-1}) and the hepatic blood flow index (HBFI, min^{-1}). K_1 here was denoted by K_u in our previous paper.[11] Details of the method are described in our previous paper.[11,15] In brief, ^{99m}Tc-GSA radioactivity in the liver at a given time t [$C^s(t)$] was initially modeled as a convolution of the blood input function [$C_b(t)$] with the sum of k exponential terms as:

$$C^{v}(t) = \sum_{i=0}^{k} \alpha_i \cdot \int_0^t C_b(u) e^{-\beta_i (t-u)} du \qquad \text{Eq. 1}$$

where α_i and β_i are assumed to be positive or zero, and are expressed in units of min^{-1}. The upper limit, k, is the maximal number of exponential terms to be included in the model and it was set at 1000. The α_i values were determined from Equation 1 and the time-activity curve of the liver by the non-negative least-squares method,[11] for β_i ranging from 0 to 1 min^{-1} with increments of 0.001 min^{-1}. From Equation 1, K_1 was given by[11]

$$K_1 = \sum_{i=0}^{k} \alpha_i - \alpha_k \qquad \text{Eq. 2}$$

where α_k represents the highest frequency component of the spectrum obtained by spectral analysis.[11] On the other hand, HEF was obtained by[15]

$$HEF = \frac{\sum_{i=0}^{k} \alpha_i - \alpha_k}{\sum_{i=0}^{k} \alpha_i} \qquad \text{Eq. 3}$$

From the relationship: $K_1 = HEF \times HBFI$, and Equations 2 and 3, the HBFI value was obtained by

$$HBFI = \sum_{i=0}^{k} \alpha_i \qquad \text{Eq. 4}$$

The HBFI value given by Equation 4 corresponds to the initial height of the tissue impulse response function.[16] This value corresponds to the blood flow perfusing the vascular space and tissue.[16]

Calculation of HH15 and LHL15

The index of blood clearance (HH15) and receptor index (LHL15) were also calculated from the time-activity curves of the liver and heart.[17,18] The HH15 value was calculated by dividing the amount of radioactivity of the heart ROI 15 min after the injection of ^{99m}Tc-GSA by that at 3 min. The LHL15 was calculated by dividing the amount of radioactivity in the liver ROI by that in the liver plus heart ROIs 15 min after the injection.

Calculation of radiation dose and volume

Because the dose per fraction and the overall duration of radiation therapy given to the 20 patients varied, the normalized total dose at a fraction size of 2 Gy (NTD – 2 Gy) was calculated for comparison.[19,20] NTD – 2 Gy was defined as

$$NTD - 2\ Gy = D \frac{\alpha/\beta + d}{\alpha/\beta + 2} \qquad \text{Eq. 5}$$

where D and d denote total dose and fraction size, respectively. Equation 5 was derived from the linear-quadratic model.[19] This can describe the response of late reacting tissue to fractionated radiation therapy when the isoeffect dose for the standard fractionation scheme of 2 Gy fractions is obtained once each day for 5 days per week.[20] Although the parameter α/β has not yet been clarified, an estimate of $\alpha/\beta = 3$ Gy for late reacting tissue has been widely applied. We therefore used 3 Gy for α/β in this

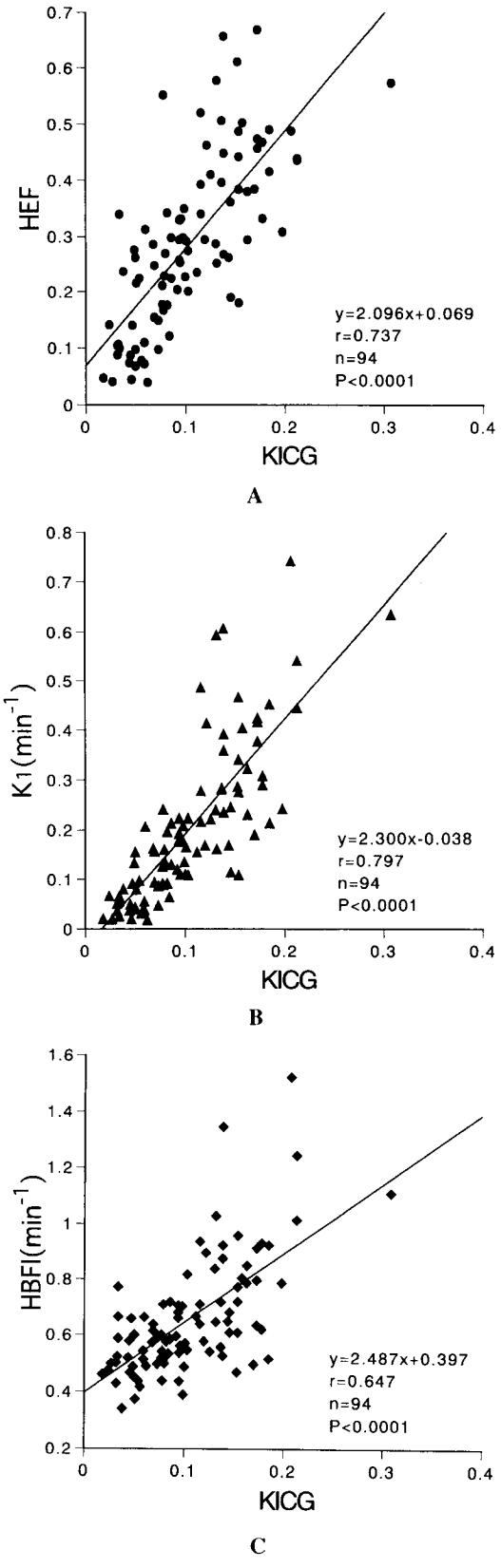

Fig. 1 Relationships between hepatic extraction fraction (HEF) and plasma disappearance rate of indocyanine green (KICG) (A), between the rate constant for liver uptake of tracer from blood (K_1) and KICG (B), and between hepatic blood flow index (HBFI) and KICG (C).

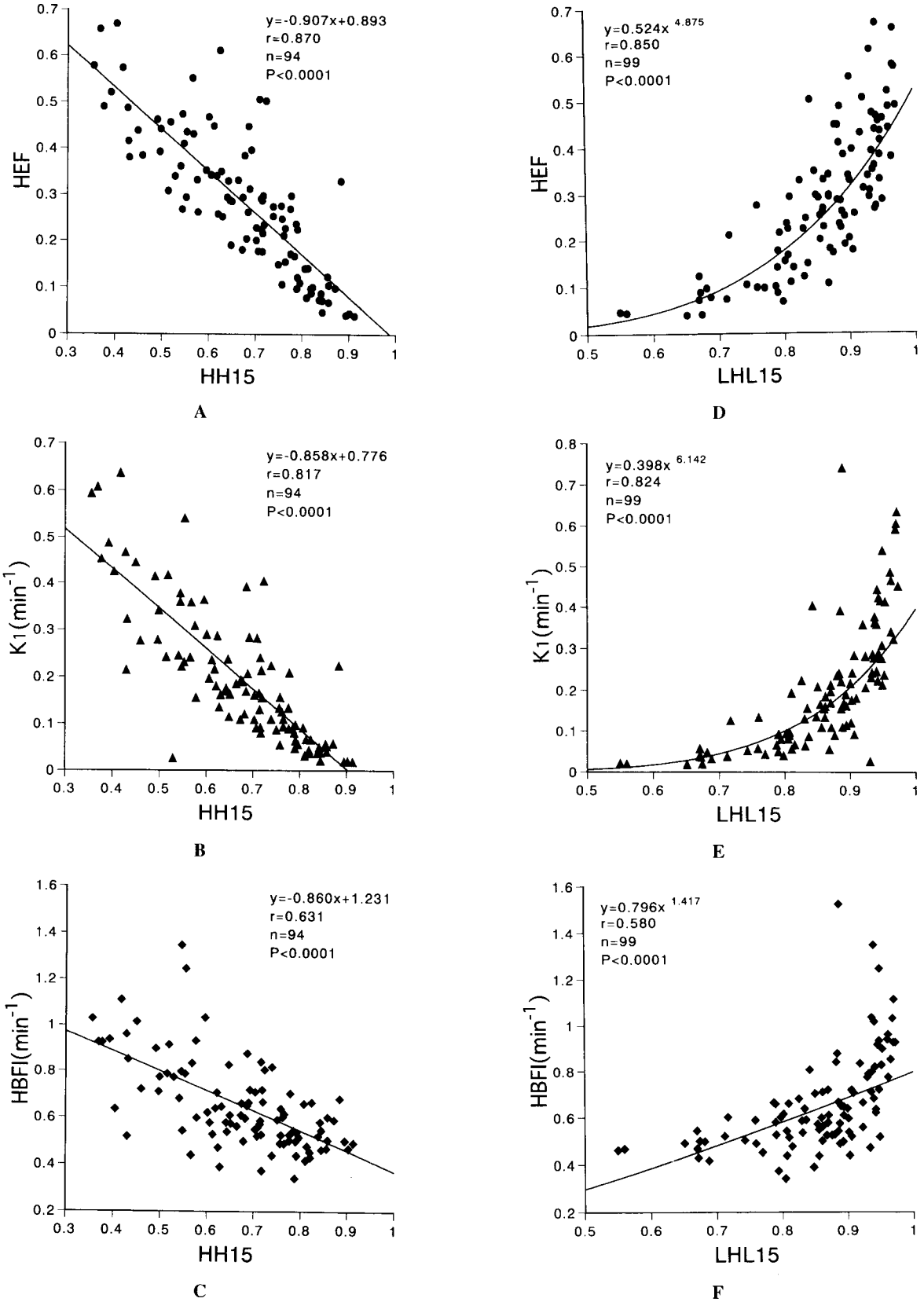

Fig. 2 Relationships between HEF and blood clearance index (HH15) (A), K_1 and HH15 (B), HBFI and HH15 (C), HEF and the receptor index (LHL15) (D), K_1 and LHL15 (E), HBFI and LHL15 (F).

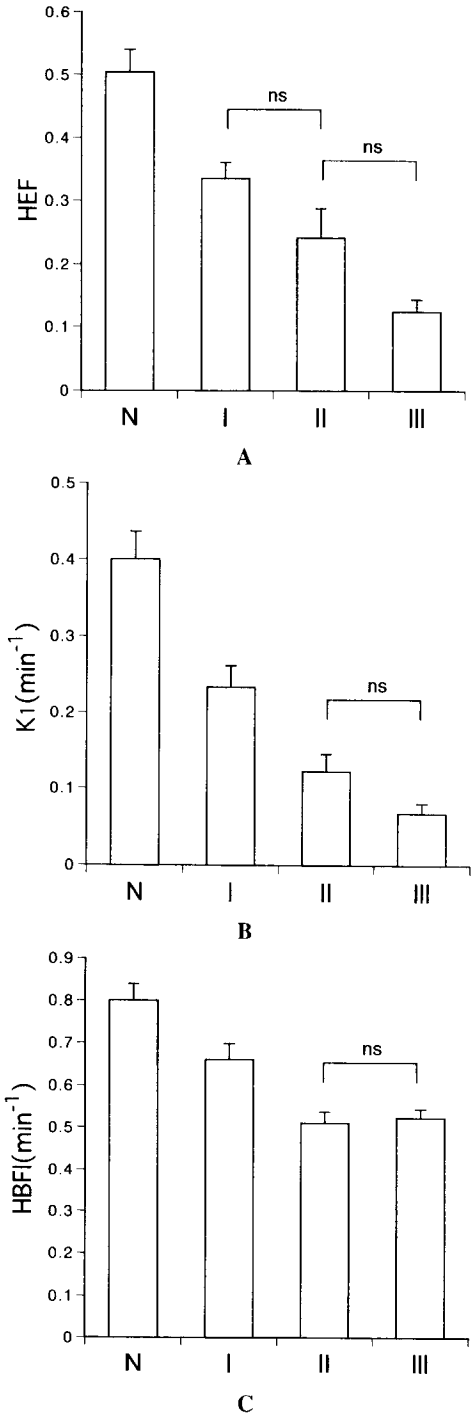

Fig. 3 Comparison of parameters between groups with normal and diseased livers. (A) HEF values. (B) K_I values. (C) HBFI values. N, I, II and III represent the patient group with no history of liver disease, mild liver dysfunction, moderate liver dysfunction and severe liver dysfunction, respectively. ns means not significant.

study. Scintigraphy with ^{99m}Tc-GSA was performed between 20 and 60 Gy, and 1 or 2 months after radiation therapy was completed in 6 patients. The average number of ^{99m}Tc-GSA scintigraphy sessions for each patient was 2.95.

Treatment was planned with a CT scan (CTS, Shimadzu, Japan) in the treatment position and the dose distribution was calculated with a treatment-planning computer (PLATO, Nucletron, Holland). The radiation dose for the liver was analyzed with histograms relating to the dose and volume, and the irradiated volume over 30% of the planned dose was taken as the irradiated volume. The irradiated liver volume ranged from 50.3 m*l* to 536.4 m*l* [288.2 ± 28.2 m*l* (mean ± S.E.)].

When analyzing changes in liver function caused by irradiation, the %change in the parameters after irradiation was calculated by taking the values before irradiation as 100% (Table 3, Figs. 4 and 5).

Biochemical tests

The results of the indocyanine green (ICG) test were compared with the results obtained with ^{99m}Tc-GSA. Blood samples were taken 5, 10 and 15 min after the intravenous injection of ICG (0.5 mg/kg body weight), and the plasma disappearance rate (KICG) was obtained. In addition, the hepaplastin test (HPT) was applied and prothrombin time (PT), total bilirubin (T.B.), total protein (T.P.), albumin (Alb) and cholinesterase (ChE) were simultaneously measured.

Statistical analysis

The correlations of the HEF, K_I and HBFI values with various liver function tests were examined by linear regression analysis (Table 1, Fig. 1). Correlations with HH15 were also analyzed by linear regression analysis (Fig. 2), whereas those with LHL15 were analyzed by the power regression equation (Fig. 2). The statistical significance of the observed differences in the values or %change in HEF, K_I and HBFI between groups was evaluated by the Mann-Whitney U test (Figs. 3, 4 and 5). A p-value below 0.05 was considered significant.

RESULTS

Table 1 summarizes correlations between the HEF, K_I and HBFI values and conventional liver function tests. Correlation was significant except between HBFI and T.B., HEF and T.P., K_I and T.P. and between HBFI and T.P. The HEF, K_I and HBFI values (y) were generally correlated in a linear fashion with KICG (x) ($y = 2.096x + 0.069$, $r = 0.737$ for HEF; $y = 2.300x - 0.038$, $r = 0.797$ for K_I; $y = 2.487x + 0.397$, $r = 0.647$ for HBFI) (Fig. 1). The correlation coefficient between K_I and KICG was the closest.

Figure 2 shows how the HEF, K_I and HBFI values correlate with HH15 and LHL15. The HEF, K_I and HBFI values were completely correlated with HH15 in a linear fashion ($y = -0.907x + 0.893$, $r = 0.870$ for HEF; $y = -0.858x + 0.776$, $r = 0.817$ for K_I, $y = -0.860x + 1.231$, $r = 0.631$ for HBFI), but nonlinearly correlated with LHL15 ($y = 0.524x^{4.875}$, $r = 0.850$ for HEF; $y = 0.398x^{6.142}$, $r = 0.824$ for K_I, $y = 0.796x^{1.417}$, $r = 0.580$ for HBFI). The

Table 2 Summary of 20 patients who underwent radiation therapy, and their hepatic extraction fraction (HEF), rate constant for the liver uptake of the tracer from the blood (K_1), and hepatic blood flow index (HBFI) values before irradiation

Patient no.	Age	Sex (M/F)	Diagnosis	NL/LC	HEF	K_1 (min^{-1})	HBFI (min^{-1})
1	77	M	Esophageal cancer	NL	0.466	0.423	0.906
2	59	F	Malignant lymphoma	NL	0.253	0.205	0.811
3	57	F	Bone metastasis	NL	0.481	0.313	0.650
4	62	M	Bone metastasis	NL	0.367	0.393	1.070
5	62	F	Lymph node metastasis	NL	0.558	0.525	0.941
6	74	F	Lung cancer	NL	0.418	0.361	0.863
7	40	F	Lymph node metastasis	NL	0.520	0.593	1.140
8	78	M	Bone metastasis	NL	0.405	0.429	1.058
9	78	M	Cholangioma	NL	0.375	0.372	0.990
10	65	F	Bone metastasis	NL	0.756	0.522	0.690
11	74	F	Lymph node metastasis	NL	0.367	0.339	0.925
12	53	F	Hepatoma	NL	0.476	0.561	1.179
13	69	F	Leukemia	NL	0.531	0.485	0.913
14	61	M	Bone metastasis	LC	0.576	0.760	1.318
15	69	M	Hepatoma	LC	0.507	0.237	0.467
16	76	F	Hepatoma	LC	0.236	0.122	0.516
17	55	M	Hepatoma	LC	0.179	0.086	0.480
18	77	F	Cholangioma	LC	0.442	0.260	0.589
19	71	M	Hepatoma	LC	0.488	0.156	0.320
20	76	M	Hepatoma	LC	0.770	0.476	0.618

NL = normal liver group; LC = liver cirrhosis group; HEF = hepatic extraction fraction; K_1 = rate constant for the liver uptake of the tracer from the blood; HBFI = hepatic blood flow index; M = male; F = female

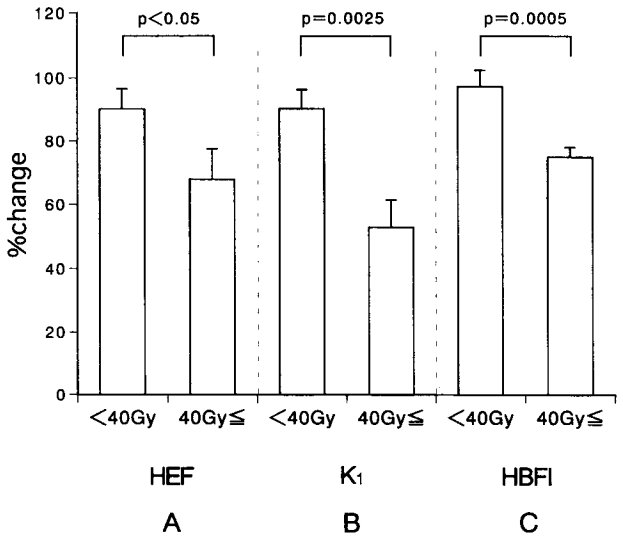

Fig. 4 Percent change of HEF (A), K_1 (B) and HBFI (C) values at doses below (< 40 Gy) and at or above 40 Gy (40 Gy ≤). Columns and horizontal bars represent means and standard error bars, respectively.

LHL15 value tended to be distributed in the upper range, whereas the distribution of the HEF and K_1 values tended to be wide during the early stage of liver dysfunction. The nonlinear relationship was more conspicuous between HEF and LHL15 and between K_1 and LHL15 than between HBFI and LHL15.

Figure 3 shows the comparisons of the HEF, K_1 and HBFI values for patients without any history of liver disease and those with various liver diseases. The HEF values were 0.504 ± 0.036 (mean ± S.E.), 0.335 ± 0.260, 0.242 ± 0.046 and 0.124 ± 0.020 for the N, I, II and III groups, respectively. The difference between groups was significant except between I and II, and between II and III. The K_1 values were 0.400 ± 0.036 min^{-1} (mean ± S.E.), 0.233 ± 0.028 min^{-1}, 0.122 ± 0.023 min^{-1} and 0.067 ± 0.013 min^{-1} for the N, I, II and III groups, respectively. The difference between the groups was significant except between II and III. The HBFI values were 0.800 ± 0.039 min^{-1} (mean ± S.E.), 0.660 ± 0.038 min^{-1}, 0.510 ± 0.027 min^{-1} and 0.523 ± 0.021 min^{-1} for the N, I, II and III groups, respectively. The difference between all groups was significant except between II and III.

Table 2 shows a summary of 20 patients who underwent radiation therapy, and their HEF, K_1 and HBFI values before irradiation. Table 3 shows the %change in the HEF, K_1 and HBFI values for the irradiated liver. All parameters tended to decrease with increasing radiation dose. Figure 4 shows a significant difference in all parameters between the values at doses below 40 Gy and those at a dose of 40 Gy or greater [%change in HEF, 90.3 ± 6.3% (mean ± S.E.) for dose < 40 Gy, 67.9 ± 9.6% for dose ≥ 40 Gy, $p < 0.05$; %change in K_1, 90.4 ± 6.1% for dose < 40 Gy, 52.9 ± 8.6% for dose ≥ 40 Gy, $p = 0.0025$; %change in HBFI, 97.4 ± 5.0% for dose < 40 Gy, 75.0 ± 3.1% for dose ≥ 40 Gy, $p = 0.0005$].

Figure 5 shows that when the radiation dose was below 40 Gy, the %change in the HEF value was more remarkable in the liver cirrhosis group than in the normal group

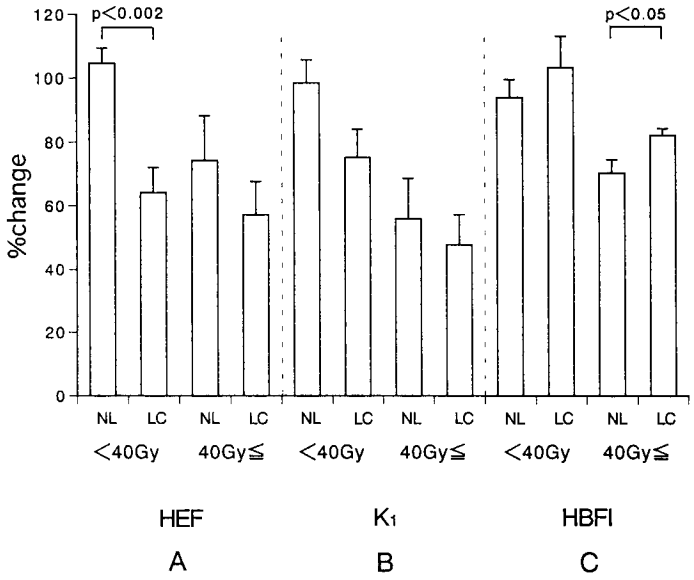

Fig. 5 Percent change in the HEF (A), K_1 (B) and HBFI (C) values of normal liver (NL) and liver cirrhosis (LC) groups at doses below (< 40 Gy) and at 40 Gy or greater (40 Gy ≤). Columns and horizontal bars represent means and standard errors, respectively.

[64.2 ± 8.0% (mean ± S.E.) and 104.6 ± 4.7%, respectively]. The difference between them was statistically significant ($p < 0.002$). On the other hand, when the dose was 40 Gy or greater, the %change in the HBFI value was more remarkable in the normal group than in the group with liver cirrhosis [70.5 ± 4.3% (mean ± S.E.) and 82.4 ± 2.1%, respectively]. The difference between them was statistically significant ($p < 0.05$). There was no significant difference between the two groups in the irradiated doses and volume.

One or two months after radiation therapy had been completed, the three parameters for 4 patients who received more than 46 Gy decreased noticeably (patients 6, 11 and 15 in Table 3) except for the HBFI value for one patient who received 50 Gy (patient 12 in Table 3). In contrast, those of the patient who received 21.6 Gy recovered completely (patient 13 in Table 3).

DISCUSSION

^{99m}Tc-GSA is a receptor-binding ligand that binds to the ASGP receptor itself specifically, which is exclusively located on the surface of hepatocytes. Numbers of this receptor decrease during liver dysfunction.[1–6] Since the target organ for ^{99m}Tc-GSA is only the liver, it is considered that the sum of liver radioactivity and blood pool radioactivity represents the total amount injected. Therefore, liver function can be accurately evaluated by measuring ^{99m}Tc-GSA kinetics. Although various methods have been proposed to obtain the indices that reflect liver functions, they have not always been applicable to routine clinical use because of complicated procedures, such as blood sampling and/or labor intensive calculation.[7–9]

Spectral analysis was first introduced for analyzing the kinetics of tracers used in a dynamic PET study.[10] This method provides information about the behavior of the tracer, such as the spectrum of the kinetic components involved in the regional uptake or partitioning of a tracer from blood to tissue and the tissue impulse response function, with minimal modeling assumptions.[10] The starting point of this method is the assumption of linear tracer kinetics to describe the kinetic behavior of the tracer. Although the kinetic behavior of ^{99m}Tc-GSA in the liver is basically nonlinear,[7–9] spectral analysis can quantify liver scintigraphy with ^{99m}Tc-GSA.[11] HEF, K_1 and HBFI values in the present study were calculated by our method based on spectral analysis as indices to represent liver functions. When spectral analysis was applied to liver scintigraphy with ^{99m}Tc-GSA, two frequency components were obtained.[11] A high frequency component is considered to result from the rapid transit time of the tracer in the vascular and/or extravascular space within the ROI (V), whereas a low frequency component is considered to result from tracer trapped in the tissue (T). Since HEF is defined as $HEF = T/(T + V)$,[15] HEF can be obtained from Equation 3. On the other hand, since K_1 and HBFI correspond to the initial values of T and T + V, respectively, when $C_b(t)$ in Equation 1 is replaced by Dirac's delta function,[15,16] these values can be obtained from Equations 2 and 4, respectively. These three parameters have the relationship: $K_1 = HEF \times HBFI$. The HEF value can be regarded as a parameter that reflects hepatocellular function (the number or activity of receptors) and capillary permeability, so that K_1 can be considered to reflect comprehensive liver function including hepatic blood flow.

Table 1 shows that HEF, K_1 and HBFI all have moderate to strong correlations with the results of various biochemical tests. The results of regression analysis showed that these parameters correlate well with KICG, which is considered to provide the best estimate of hepatic reserve capacity (defined by the total number of

Table 3 Change of the hepatic extraction fraction (HEF), the rate constant for the liver uptake of the tracer from the blood (K_1), and the hepatic blood flow index (HBFI) values of the irradiated liver

Patient no.	V (m*l*)	D (Gy)	20 Gy ≤ dose < 30 Gy			30 Gy ≤ dose < 40 Gy			40 Gy ≤ dose < 50 Gy			50 Gy ≤			1–2 months later		
			HEF (%)	K_1 (%)	HBFI (%)	HEF (%)	K_1 (%)	HBFI (%)	HEF (%)	K_1 (%)	HBFI (%)	HEF (%)	K_1 (%)	HBFI (%)	HEF (%)	K_1 (%)	HBFI (%)
1	50.3	2.0							102.7	88.0	85.7	43.9	29.7	67.9			
2	75.2	2.0							33.0	20.6	62.5	14.0	8.0	57.3			
3	349.5	2.0				107.2	103.6	96.8									
4	278.3	2.0				117.2	112.3	95.9				44.5	30.4	72.9			
5	248.5	2.0	81.5	51.0	62.8				48.1	22.6	46.8				34.3	21.2	61.9
6	334.8	2.0	140.3	134.9	96.1							88.0	69.9	79.9	20.8	13.1	62.7
7	288.8	1.8	89.0	101.5	113.7												
8	254.3	3.0				104.0	81.0	77.9									
9	471.7	2.0				113.7	104.5	92.0	90.3	60.2	66.7						
10	536.4	3.0				98.7	95.9	97.2									
11	127.0	2.0				98.2	131.0	113.3	137.5	128.0	93.0				51.3	35.4	69.0
12	332.3	2.0				104.8	81.0	77.3				141.2	102.2	72.4	72.8	53.7	73.7
13	273.0	1.5	95.9	87.7	91.5										108.5	115.6	106.6
14	143.1	3.0										57.7	41.9	73.4			
15	200.5	2.0				76.3	76.0	99.6				64.5	52.3	81.0	11.3	42.2	53.3
16	296.3	3.0				66.3	54.8	76.0				92.9	84.7	83.8			
17	382.1	2.0				40.0	85.8	93.2									
18	320.6	1.8	90.4	88.4	97.7				70.1	57.1	81.4						
19	444.6	3.0				42.7	45.3	106.1				17.2	14.9	86.7			
20	357.6	2.0	69.2	101.7	148.0							40.5	35.6	87.8			

V = irradiated volume (m*l*); D = dose per fraction (Gy); Gy = normalized total dose at a fraction size of 2 Gy (NTD – 2 Gy); HEF = hepatic extraction fraction; K_1 = rate constant for the liver uptake of the tracer from the blood; HBFI = hepatic blood flow index

The numbers in the table represent the %change after irradiation when taking the value before irradiation as 100%.

functioning hepatocytes) among conventional tests (Fig. 1). Furthermore, the correlations between HEF or K_1 and biochemical tests were better than those between HBFI and the same tests. These results suggest that the HEF or K_1 values obtained by our method are more closely related to liver function reflecting the total number of functioning hepatocytes than the HBFI value. This also indicates that our method can evaluate liver function separately from hepatic blood flow.

HH15 and LHL15 are useful indices that can be simply obtained. HH15 represents the retention of the tracer in the blood, and LHL15 illustrates the hepatic uptake of the tracer from blood, and can evaluate liver function in the clinical setting.[17,18] The HEF, K_1 and HBFI values obtained by our method were almost totally correlated in a linear fashion with HH15 (Fig. 2). On the other hand, correlations with LHL15 were not linear, which was more noticeable in HEF and K_1 than in HBFI (Fig. 2). LHL15 was densely located in the upper range, whereas the parameters obtained by our method were widely distributed. This implies that the parameters obtained by our method (especially HEF and K_1) are more sensitive to liver damage than LHL15, especially during the early stage of liver dysfunction. The relationship between LHL15 and HEF, and LHL15 and K_1 resembles that of LHL15 and the maximal receptor binding rate (Rmax) that was derived from compartment analysis by Ha-Kawa et al.[8] From this we can conclude that HEF and K_1 are closely related to Rmax.

As shown in Figure 3, the HEF, K_1 and HBFI values obtained by our method decreased as the severity of liver dysfunction progressed, implying that they can evaluate the severity of liver dysfunction. Although there was no significant difference between the moderate and severe dysfunction groups for all parameters, the HEF and K_1 values tended to decrease gradually according to the severity of liver dysfunction. Nevertheless, the change in the HBFI value was relatively small and the difference between the moderate and severe dysfunction groups was almost negligible. Therefore it can be suggested that K_1 is the superior parameter for describing comprehensive liver function. This notion is also supported by the results shown in Table 1.

One of the advantages of our method is that regional liver function can be evaluated by setting an ROI to a portion of the liver. When radiation therapy was applied to anterior/posterior or anteroposterior opposite portals, an ROI could be drawn over the irradiated region of the liver. After that, changes in the above parameters due to irradiation could be evaluated.

The radiation tolerance of the liver has not yet been completely clarified. Radiation damage to the liver is called radiation hepatitis, and is characterized by features such as liver dysfunction, hepatomegaly and ascites, and it has been defined as a veno-occlusive disease.[21,22] It is estimated that whole liver irradiation with 30 to 35 Gy is tolerable, but more substantial irradiation is possible, if it is partial. There are many uncertain aspects regarding the effects of irradiation on liver function. To our knowledge, the effects of irradiation on regional function of the liver have not been quantified.

All parameters obtained from the irradiated liver by our method tended to decrease with increasing radiation dose (Fig. 4), but the HEF and HBFI values did not always change in parallel, and sometimes they increased regardless of irradiation (Table 3). As shown in Figure 5, when the radiation dose was 40 Gy or greater, the decreased HBFI values were more apparent in patients without, than with liver cirrhosis. On the other hand, when the dose was less than 40 Gy, the decreases in HEF were more significant in patients with, than without liver cirrhosis. These results imply that the degree of change in HEF and HBFI is influenced by the condition of the liver, that is, whether or not cirrhosis is present.

Damage to blood vessels is the most conspicuous effect of irradiation of the liver, as the formation of fibrin mesh and/or fibrosis in the sinusoid or central veins is caused by damaged endothelial cells, and gross morphology shows severe congestion of the liver with edema and hyperemia.[23] In patients with liver cirrhosis, hepatic blood flow decreases due to periportal fibrosis, and the component of the blood supply from arteries relatively increases. When peripheral vaso-occlusion occurs in the irradiated liver, the blood flow in the portal vein decreases before that in the arteries due to the vein's lower blood pressure. As a result, total hepatic blood flow appears to rapidly decrease in the normal liver. On the other hand, the decrease in total hepatic blood flow is not so rapid in the cirrhotic liver, because the proportion of the blood supply from the portal vein is relatively small and the arteries may also compensate. This appears to be the main reason why the decrease in HBFI in patients without liver cirrhosis is more noticeable than that in patients with liver cirrhosis at a dose of 40 Gy or greater (Fig. 5).

Animal experiments show that capillary permeability increases without significant morphological change other than edema soon after irradiation,[24] so that a lot of tracer may accumulate on the outside of vessels. It is known that HEF is closely related to capillary permeability and hepatocellular function (number or activity of receptors). Therefore it is considered that the tracer is effectively taken up by hepatocytes in the normal liver where receptors are retained well at a low radiation dose. Nevertheless, we must consider, since the decrease in the number or activity of receptors is noticeable in the cirrhotic liver, the decrease in HEF might be noticeable despite increased vessel permeability. This may be one reason why the decrease in the HEF value in patients with liver cirrhosis is significantly greater than that in those without this condition at a dose below 40 Gy (Fig. 5).

Late changes in the irradiated liver are characterized by atrophy and fibrosis.[23] In this study, all indices except for

the HBFI of one patient were reduced in patients who received more than 46 Gy, whereas all parameters of the patient who received 21.6 Gy recovered 1 or 2 months after radiation therapy was completed (Table 3). These results suggest that the dysfunction caused by irradiation is reversible at least at low doses, but further studies on the irradiated region or volume will be needed to define changes in liver function during or after irradiation.

Our method can be applied to dynamic SPECT[25] with minor modifications. This will allow changes in regional liver function due to irradiation to be evaluated in a three-dimensional manner.

CONCLUSIONS

Quantitative evaluation of dynamic liver scintigraphy with ^{99m}Tc-GSA by means of spectral analysis is a simple and noninvasive method that can separately evaluate hepatocellular function and hepatic blood flow. Furthermore, regional change in these parameters in the irradiated liver can be estimated by this method.

REFERENCES

1. Morell AG, Irvine RA, Sternlieb I, Scheunberg IH, Ashwell G. Physical and chemical studies on ceruloplasmin. V. Metabolic studies on sialic acid free ceruloplasmin *in vivo*. *J Biol Chem* 243: 155–159, 1968.
2. Pricer WE, Ashwell G. The binding of desialylated glycoproteins by plasma membranes of liver. *J Biol Chem* 246: 4825–4833, 1971.
3. Ashwell G, Morell AG. The role of surface carbohydrates in the hepatic recognition and transport of circulating glycoproteins. *Adv Enzymol* 41: 99–128, 1974.
4. Stochert RJ, Becker FF. Diminished hepatic binding protein for disialylated glycoproteins during chemical hepatocarcinogenesis. *Cancer Res* 40: 3632–3634, 1980.
5. Sawamura T, Kawasato S, Shiozaki Y, Samesima Y, Nakada H, Tashiro Y. Decrease of a hepatic binding protein specific for asialoglycoproteins with accumulation of serum asialoglycoproteins in galactosamine-treated rats. *Gastroenterology* 81: 527–533, 1981.
6. Sawamura T, Nakada H, Hazama Y, Shiozaki Y, Samesima T, Tashiro Y. Hyperasialoglycoproteinemia in patients with chronic liver diseases and/or liver cell carcinoma. *Gastroenterology* 87: 1217–1221, 1984.
7. Vera DR, Stadalnik RC, Trudeau WL, Scheibe PO, Krohn KA. Measurement of receptor concentration and forward-binding rate constant via radiopharmacokinetic modeling of technetium-99m-galactosyl-neoglycoalbumin. *J Nucl Med* 32: 1169–1176, 1991.
8. Ha-Kawa SK, Tanaka Y. A quantitative model of technetium-99m-DTPA-galactosyl-HAS for assessment of hepatic blood flow and hepatic binding protein. *J Nucl Med* 32: 2233–2240, 1991.
9. Miki K, Kubota K, Kokubo N, Inoue Y, Bandai Y, Makuuchi M. Asialoglycoprotein receptor and hepatic blood flow using technetium-99m-DTPA-galactosyl human serum albumin. *J Nucl Med* 38: 1798–1807, 1997.
10. Cunningham VJ, Jones T. Spectral analysis of dynamic PET studies. *J Cereb Blood Flow Metab* 13: 15–23, 1993.
11. Murase K, Tsuda T, Mochizuki T, Ikezoe J. A simplified method for the quantitative analysis of ^{99}Tc^{m}-GSA liver scintigraphy using spectral analysis. *Nucl Med Commun* 18: 1049–1056, 1997.
12. Ohara K, Sugahara S, Yoshida T, Matsueda K, Kuramoto K, Akisada M. Radiation tolerance of partially irradiated liver in a multidisciprinary treatment for hepatoma. *Nippon Acta Radiologica* 50: 146–154, 1990.
13. Tsuji H, Okumura T, Maruhashi A, Hayakawa Y, Matsuzaki Y, Tanaka N, et al. Dose-volume histogram analysis of patients with hepatocellular carcinoma regarding changes in liver function after proton therapy. *Nippon Acta Radiologica* 55: 322–328, 1995.
14. Liver Cancer Study Group of Japan. *The general rules for the clinical and pathological study of primary liver cancer*. 3rd ed., Tokyo, Kanehara Publishing Co., p. 20, 1992.
15. Murase K, Tsuda T, Mochizuki T, Ikezoe J. Hepatic extraction fraction of hepatobiliary radiopharmaceuticals measured using spectral analysis. *Nucl Med Commun* 20: 1041–1045, 1999.
16. Murase K, Inoue T, Fujioka H, Ishimaru Y, Akamune A, Yamamoto Y, et al. An alternative approach to estimation of the brain perfusion index for measurement of cerebral blood flow using technetium-99m compounds. *Eur J Nucl Med* 26: 1333–1339, 1999.
17. Torizuka K, Ha-Kawa SK, Kudo M, Kubota Y, Yamamoto K, Itoh K, et al. Phase III multicenter clinical study on Tc-99m GSA, a new agent for functional imaging of the liver. *KAKU IGAKU (Jpn J Nucl Med)* 29: 159–181, 1992.
18. Kudo M, Todo A, Ikekubo K, Hino M, Yonekura Y, Yamamoto K, et al. Functional hepatic imaging with receptor-binding radiopharmaceutical: Clinical potential as a measure of functioning hepatocytes mass. *Gastroenterology Jpn* 26: 734–741, 1991.
19. Yaes RJ, Patel P, Maruyama Y. On using the Linear-Quadratic model in daily clinical practice. *Int J Radiat Oncol Biol Phys* 20: 1353–1362, 1991.
20. Nishimura Y. Late damages associated with high-dose rate intraluminal brachytherapy and radiation therapy treating only one field each day—analysis by the linear-quadratic model (NTD – 2 Gy)—. *J Jpn Soc Ther Radiol Oncol* 11: 183–190, 1999.
21. Ingold JA, Reed GB, Kaplan HS, Bagshaw MA. Radiation hepatitis. *Am J Roentgenol* 93: 200–208, 1965.
22. Reed GB, Cox AJ Jr. The human liver after radiation injury: A form of venoocclusive disease. *Am J Path* 48: 597–611, 1966.
23. Trott KR, Herrmann T. Radiation effects on the liver. Scherer E, Streffer C, Trott K-R, eds., *Radiopathology of Organs and Tissues*, Berlin, Springer-Verlag, pp. 329–346, 1991.
24. Michael MG, Lanell MP. Functional measures endothelial integrity and pharmacologic modification of radiation injury. David BR, eds., *The Radiation Biology of the Vascular Endothelium*, CRC press, pp. 40–63, 1998.
25. Hwang EH, Taki J, Shuke N, Nakajima K, Kinuya S, Konishi S, et al. Preoperative assessment of residual hepatic functional reserve using ^{99m}Tc-DTPA-galactosyl-human serum albumin dynamic SPECT. *J Nucl Med* 40: 1644–1651, 1999.